

## Normal-state transport in electron-doped $\text{La}_{2-x}\text{Ce}_x\text{CuO}_4$ thin films in magnetic fields up to 40 Tesla

K. Jin,<sup>1</sup> B. Y. Zhu,<sup>1</sup> B. X. Wu,<sup>1</sup> J. Vanacken,<sup>2</sup> V. V. Moshchalkov,<sup>2</sup> B. Xu,<sup>1</sup> L. X. Cao,<sup>1</sup> X. G. Qiu,<sup>1</sup> and B. R. Zhao<sup>1,\*</sup>

<sup>1</sup>National Laboratory for Superconductivity, Institute of Physics, and Beijing National Laboratory for Condensed Matter Physics, Chinese Academy of Sciences, Beijing 100080, People's Republic China

<sup>2</sup>INPAC-Institute for Nanoscale Physics and Chemistry, K. U. Leuven, Celestijnenlaan 200D, B-3001 Leuven, Belgium

(Received 21 February 2008; published 12 May 2008)

The in-plane normal-state transport properties of electron-doped superconductor  $(\text{La}_{2-x}\text{Ce}_x)\text{CuO}_4$  (LCCO) thin films with  $0.06 \leq x \leq 0.17$  are studied in magnetic fields up to 40 Tesla. For the whole doping region investigated, the negative magnetoresistivity ( $n$ -MR) is found below certain temperatures, with minimum  $n$ -MR near the optimal doping (0.10–0.11). In the superconducting region ( $x=0.09$ –0.17), all the LCCO films show crossover from positive MR to  $n$ -MR. For  $x=0.09$ , the magnetic field corresponding to the crossover from positive MR to  $n$ -MR shows a parabolic behavior with varying temperature. For  $x=0.12$ , second crossing point of  $\rho(B, T)$  curves is observed by tuning the magnetic field.

DOI: 10.1103/PhysRevB.77.172503

PACS number(s): 74.25.Fy, 74.40.+k, 74.72.-h

Studying the normal-state transport behavior by suppressing the superconductivity with high magnetic fields is an effective method to gain an insight into the intrinsic features of high- $T_c$  superconductors (HTSCs).<sup>1–7</sup> So far, such investigations are mostly focused on the underdoped  $p$ -type cuprates, such as  $\text{La}_{2-x}\text{Sr}_x\text{CuO}_4$ ,<sup>1</sup>  $\text{Bi}_2\text{Sr}_2\text{CaCu}_2\text{O}_{8+x}$ ,<sup>2</sup> and  $\text{YBa}_2\text{Cu}_3\text{O}_{6+x}$  (Ref. 4) systems, since for the superconductors with nearly optimal doping level, the upper critical magnetic field  $B_{c2}$  (order of  $\sim 100$  Tesla)<sup>8</sup> is too high to be achieved. The  $n$ -type HTSCs have relatively lower  $B_{c2}$  (order of  $\sim 10$  Tesla),<sup>9,10</sup> so their superconductivity is easier to be suppressed to look into the normal-state properties and the magnetoresistivity naturally becomes the first effect to be studied. For example, recently, the low temperature longitudinal negative magnetoresistivity ( $n$ -MR) has been investigated for  $\text{Nd}_{2-x}\text{Ce}_x\text{CuO}_4$  (NCCO) and  $\text{Pr}_{2-x}\text{Ce}_x\text{CuO}_4$  (PCCO) systems.<sup>7,11</sup> Further, it should be noted that the  $n$ -type HTSCs have their own special features compared to the  $p$ -type counterparts, such as the Fermi surface evolving with doping due to the existence of both electronlike and holelike charge carriers,<sup>12</sup> the in-plane resistivity obeying the two-dimensional (2D) Fermi liquid model under the optimal- and overdoping levels.<sup>13</sup> Therefore, the study of the normal-state properties in high magnetic fields is necessary to be performed in a wide range of doping for  $n$ -type HTSC. On the other hand, the metastable phase superconductor  $\text{La}_{2-x}\text{Ce}_x\text{CuO}_4$  (LCCO), with the highest  $T_c$  so far in the  $n$ -type superconductor family,<sup>14</sup> is rarely studied compared to other  $n$ -type HTSC, especially in high magnetic fields.

Based on this consideration, the normal-state transport properties of LCCO with  $0.06 \leq x \leq 0.17$  in the magnetic fields of up to 40 Tesla are investigated in this study. The optimal doping is  $x \sim 0.10$ , which is determined by its highest zero transition temperature  $T_c$  and sharpest transition among all the LCCO thin films. All the samples show  $n$ -MR effect, and for  $x \leq 0.09$ , the  $n$ -MR effect is quite strong, while for  $x \geq 0.09$ , with increasing the magnetic field, the  $\rho(T, B)$  curves first demonstrate a positive magnetoresistivity ( $p$ -MR) that leads to the appearance of crossing point (CP) for the  $\rho(T, B)$  curves, then cross over to  $n$ -MR at certain higher fields,  $B_{pn}$ s. The minimum  $n$ -MR is observed near the

optimal doping. Moreover,  $B_{pn}$  versus temperature shows a parabolic behavior for  $x=0.09$ , and second CP is observed for  $x=0.12$  when the field is increased to  $\sim 34$  Tesla.

All the LCCO thin films were prepared by dc magnetron sputtering.<sup>15,16</sup> To obtain LCCO thin films with high quality, we carefully adjusted the deposition temperature, the ratio of Ar to  $\text{O}_2$ , and the annealing process for each doping level.<sup>17</sup> Owing to the undetermined oxygen content in films, we chose the highest  $T_c$  and sharp transition of the annealed films for each Ce content. All the films are  $c$ -axis oriented with thickness of  $\sim 1000$  Å and were patterned into the bridges with six terminals for the transport measurements in pulsed magnetic fields (0–40 Tesla) at the K. U. Leuven and in dc magnetic fields of up to 12 Tesla by using the Quantum Design PPMS-14 setup. The samples were mounted with  $B \perp ab$  plane and  $B \perp$  current  $I$ . The heating effect due to eddy current is negligible since the data obtained from both up and down sweeps of the magnetic field coincided with each other. The  $\rho(T, B)$  measurements at different fields (including  $B=0$ ) were performed for LCCO thin films with  $x=0.06, 0.08, 0.09, 0.10, 0.11, 0.12, 0.13, 0.15$ , and 0.17.

In Fig. 1, we present  $\rho(T, B)$  curves for LCCO thin films with  $x=0.09, 0.12, 0.15$ , and 0.17 and  $T_c=22.5, 19, 12$ , and 3 K, respectively. In Figs. 1(a) and 1(b), one can see that the films in the superconducting doping region with  $x=0.09$  and 0.12 tend to be insulating with increasing magnetic field. The  $\rho \propto B^2$  relation is observed in certain field range, which might be resulted from the coexistence of electronlike and holelike charge carriers near optimal doping.<sup>10</sup> Figures 1(c) and 1(d) show the  $\rho(T, B)$  data for  $x=0.15$  and 0.17, respectively, and a distinct superconductor-metal phase transition is observed. In contrast to that, the films with  $x=0.06$  and 0.08 are non-superconducting, and the insulator-metal (IM) phase transition is revealed, which starts from the minimum resistivity temperature  $T_{\min} \sim 90$  and 88 K, respectively, at zero magnetic field [see insets of Figs. 2(a) and 2(b)]. The 2D localization effects<sup>18</sup> or Kondo scattering<sup>19</sup> could be responsible for a log  $T$  resistance in zero field in these samples.

Figure 2 shows the isothermal  $\rho(B)$  curves for LCCO thin films with  $x=0.06, 0.08, 0.09, 0.12$ , and 0.15. As seen in Figs. 2(a) and 2(b), the LCCO thin films with  $x=0.06$  and

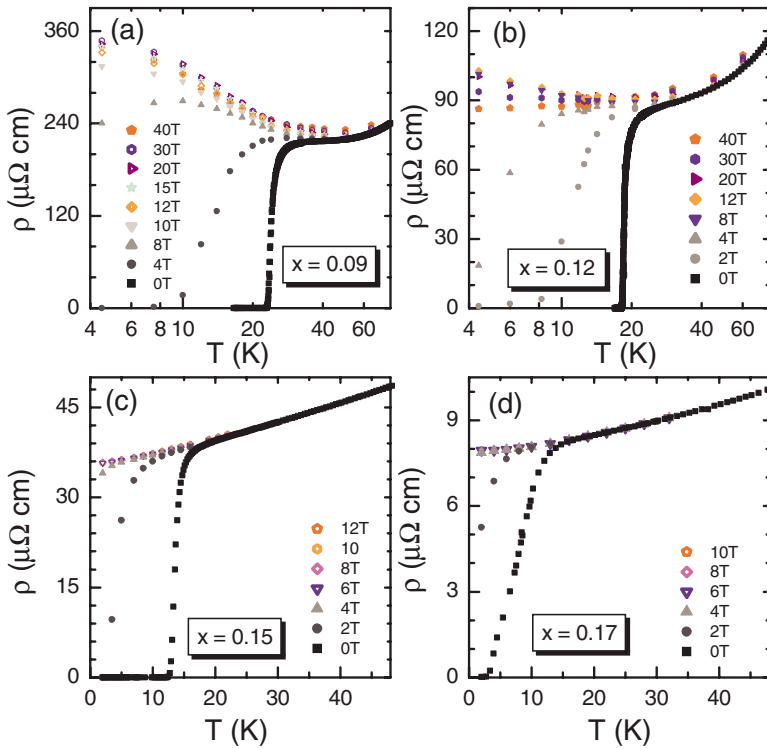


FIG. 1. (Color online) Resistivity  $\rho$  vs temperature at different fields for the LCCO with  $x$  = (a) 0.09, (b) 0.12, (c) 0.15, and (d) 0.17. Note that for  $x=0.09$  and 0.12, the  $x$  axis is plotted in logarithmic scale.

0.08 in the magnetic field show quite strong  $n$ -MR in the temperature region below  $T_{\min}$ . Now, we focus on the  $n$ -MR effect in the LCCO thin films with superconductivity suppressed by magnetic field. With increasing the magnetic field, all these superconducting films first show  $p$ -MR and then cross over to  $n$ -MR at certain magnetic fields,  $B_{pn}$ s; the  $B_{pn}$  of  $x=0.09$  particularly presents a parabolic relation with  $T$  [inset of Fig. 2(c)]. For the slightly underdoped ( $x=0.09$ )

and overdoped ( $x=0.12$ ) films, the isothermal  $\rho(B)$  curves show a CP at relatively lower fields in the  $p$ -MR region; especially, second CP is observed for  $x=0.12$  at higher field to  $\sim 34$  Tesla. This is a finding for the transport feature of such  $n$ -type HTSC.

We first focus on the relation between the  $n$ -MR effect and the doping level. The normalized MR,  $\Delta\rho(B)/\rho_{\max}$  ( $[\rho(B) - \rho_{\max}]/\rho_{\max}$ ), versus the Ce content  $x$  at 4.5 K is plot-

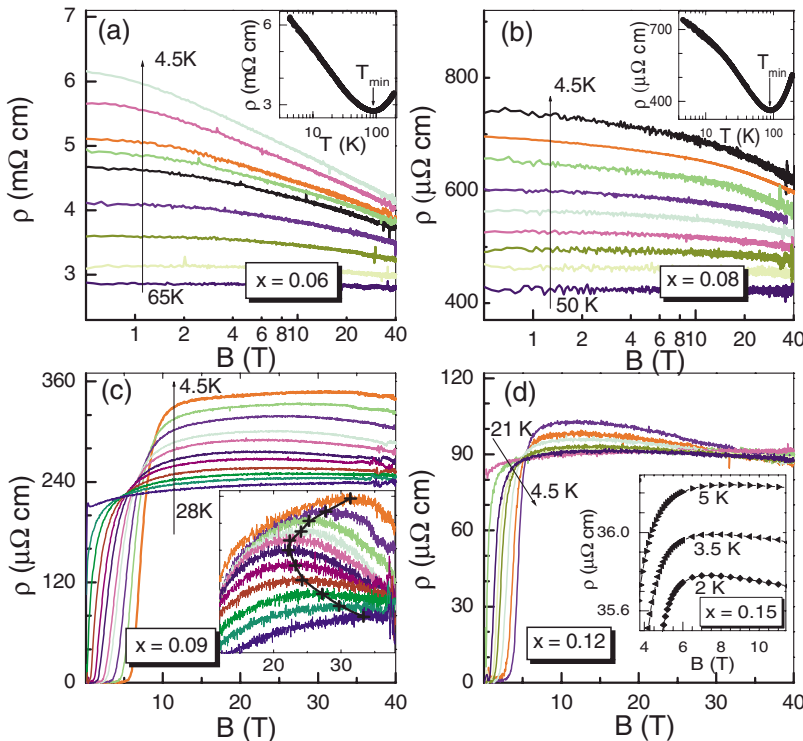


FIG. 2. (Color online) Isothermal  $\rho(B)$  curves for LCCO with  $x$ =(a) 0.06, (b) 0.08, (c) 0.09, and (d) 0.12. In (d), there is a second crossover (indicated by red arrow), which may mean a phase transition for  $x=0.12$ . The insets: zero field resistivity vs temperature for  $x$ =(a) 0.06 and (b) 0.08, enlarged  $\rho(B)$  curves for (c)  $x=0.09$ , and  $\rho(B)$  curves for (d)  $x=0.15$ . Note that for  $x=0.06$  and 0.08, the  $x$  axis is plotted in logarithmic scale.

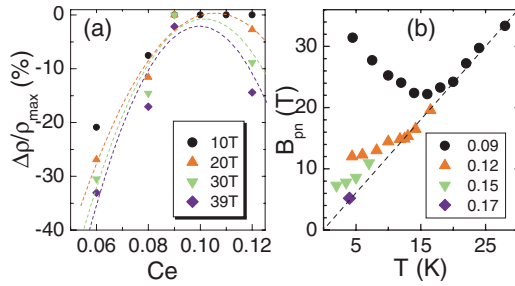


FIG. 3. (Color online) (a)  $n$ -MR vs Ce concentration at 4.5 K. (b) The  $B_{pn}$  vs temperature for the LCCO with  $x=0.09, 0.12, 0.15,$  and  $0.17$ . The onset of  $B_{pn}(T)$  for each doping level lies on the same straight line and especially the  $B_{pn}(T)$  for  $x=0.09$  shows a parabolic relation.

ted in Fig. 3(a). Here,  $\rho_{\max}$  is the maximum of  $\rho(B)$ , at which the crossover of  $p$ -MR to  $n$ -MR occurs. In order to present the  $n$ -MR effect, the MR value in the field  $B < B_{pn}$  is defined as zero. At  $B=30$  Tesla, we can see that  $\Delta\rho(B)/\rho_{\max}$  changes from  $-30\%$  ( $x=0.06$ ) to nearly zero ( $x=0.09$ ) and then to  $-10\%$  ( $x=0.12$ ). Obviously, the  $n$ -MR is stronger in the underdoped and the slightly overdoped regions, with the minimum  $n$ -MR near the optimal doping. In Fig. 3(b), we plot the  $B_{pn}$  at various temperatures for LCCO thin films in the superconducting region with  $x=0.09, 0.12, 0.15,$  and  $0.17$ . The main arguments about this can be summarized as follows: (i) the higher the  $T_c$  is, the larger the  $B_{pn}$  is; (ii) the  $B_{pn}$  decreases with decreasing temperature except that of  $x=0.09$ , which first decreases and then increases [inset of Fig. 2(a)]; (iii) for all these doping levels, the  $B_{pn}(T)$  in higher temperature region lies on the same straight dashed line, which may mean a common origin of the  $n$ -MR for the investigated LCCO thin films; (iv) the  $B_{pn}$  deviates from the dashed line at low temperatures. We note that in the electron-doped  $\text{Pr}_{2-x}\text{Ce}_x\text{CuO}_{4-\delta}$  films,  $B_{pn}$  obviously decreases with decreasing temperature for  $x=0.16$  (Ref. 7); on the contrary, the  $B_{pn}$  increases with decreasing temperature in the hole-doped  $\text{La}_{2-x}\text{Sr}_x\text{CuO}_4$  film with  $x=0.08$ .<sup>1</sup> Moreover, in  $\text{InO}_x$  films, with decreasing temperature, the  $B_{pn}$  decreases for sample with lower  $H_{c2}(0)$  (mean-field upper critical field) but increases for higher  $H_{c2}(0)$ .<sup>8</sup> Hence, we may infer that not only one reason results in the behavior of  $B_{pn}$  versus temperature, i.e., the starting of  $n$ -MR effect.

The origin of the  $n$ -MR is still under debate, as known as the delocalization,<sup>20</sup> the suppression of spin density wave (SDW) gap ( $\Delta_{SDW}$ ),<sup>21,22</sup> and the depairing of the Cooper pairs.<sup>8</sup> First, we consider the possible surviving of locally Cooper pairs due to the quantum phase fluctuation.<sup>23</sup> If localized Cooper pairs are destroyed when the magnetic field is further increased, the quasiparticles will contribute to transport, which should result in the  $n$ -MR effect.<sup>24</sup> However, the  $B_{pn}$ s are larger than the  $B_{c2}$  values for these doping levels, especially for  $x=0.09$ ,<sup>25</sup> and the lower the temperature, the harder the magnetic field is to destroy the localized Cooper pairs, that is, the  $B_{pn}$  should increase with decreasing temperature. We cannot exclude the possibility of remaining superconductivity above  $B_{pn}$  in  $x=0.12$  and  $0.15$ , which may be responsible for the deviation from the straight dashed line [Fig. 3(a)]. While, the field suppression of  $\Delta_{SDW}$  seems to be

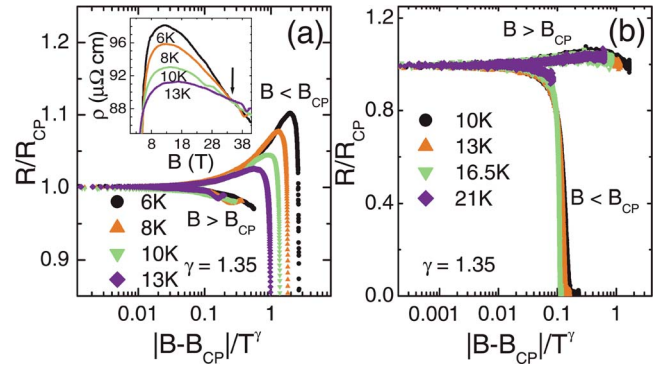


FIG. 4. (Color online) The scaling analysis of  $R/R_{cp}$  vs  $|B - B_{cp}|/T^\gamma$  for (a) the second CP and (b) the first CP for  $x=0.12$ , with  $\gamma=1.35$  and  $R_{cp} \sim 89 \mu\Omega \text{ cm}$ . The inset in (a) shows  $\rho(T_0, B)$  curves at various temperatures  $T_0$  for  $x=0.12$ .

more reasonable for the deviation from the straight dashed line, especially for  $x=0.09$ . On one hand,  $\Delta_{SDW}$  opens at certain temperature and higher fields are needed to suppress it at lower temperatures, that is, the  $B_{pn}$  increases with decreasing temperature; on the other hand, in PCCO<sup>21</sup> and NCCO,<sup>22</sup> the magnitude of this gap decreases to zero from underdoped region to  $x \sim 0.17$  and  $x < 0.15$ , respectively. Similarly, for LCCO, the deviation from the straight dashed line should be reduced with increasing doping. Then, we may find a proper explanation for the straight line behavior of  $B_{pn}(T)$  (ii). Simply, the localized charge carriers delocalize with increasing magnetic field, which causes  $n$ -MR. Meanwhile, the destroying of superconductivity, two kinds of charge carriers,<sup>10</sup> or particle-particle interaction channel will cause  $p$ -MR,<sup>20</sup> so  $B_{pn}$  appears. It is harder to suppress spin disorder at higher temperatures so that the  $B_{pn}$  may decrease with decreasing temperature. The Hall measurements prove that the optimal doped LCCO films have smallest rich oxygen or oxygen vacancy and have the highest  $T_c$ , which is why the optimal doping has the minimum  $n$ -MR. Finally, we take  $x=0.12$ , for example, to test the possible delocalization process.

The crossing point of  $\rho(B, T)$  might represent a 2D transition controlled by quantum phase fluctuations. It is known that the transport in LCCO samples is highly two-dimensional, especially near the optimal doping,<sup>13</sup> so we use the scaling law of the 2D macroscopic quantum phase coherence<sup>26,28</sup> to analyze the second CP for  $x=0.12$ , that is, the data near the CP should obey the scaling  $R(|B - B_{cp}|, T) \propto R_{cp} f(|B - B_{cp}|T^{-\gamma})$ .<sup>26,27</sup> Here,  $f(|B - B_{cp}|T^{-\gamma})$  is a dimensionless scaling function, and  $\gamma = 1/\nu z$ , with  $\nu$  and  $z$  as the correlation length and dynamical exponent, respectively.  $B_{cp}$  and  $R_{cp}$  represent the magnetic field and resistivity at CP, respectively. Figure 4(a) demonstrates that the data around the second CP  $\sim 34$  Tesla satisfy this scaling over more than two decades of  $|B - B_{cp}|T^{-\gamma}$ , with the  $R_{cp} \sim 89 \mu\Omega \text{ cm}$  and best fitting parameter  $\gamma=1.35$ . The second CP may reveal the phase transition from the localization (insulating state) to the delocalization (metallic state) of the electronic states.<sup>26,28,29</sup> It is interesting that such scaling is also satisfied for the first CP at  $\sim 5$  Tesla, as seen in Fig. 4(b), with the same  $R_{cp} \sim 89 \mu\Omega \text{ cm}$  and best fitting param-

eter  $\gamma=1.35$ . The differences are  $B_{cp}$  and the transport behavior below and above  $B_{cp}$ . It should also be noted that the scaling exponent  $\gamma=1.35$  is much larger than that for the IM transition in heavily Si-doped  $\text{Al}_{0.3}\text{Ga}_{0.7}\text{As}$ .<sup>28</sup> This is mainly due to the different nature of these materials.<sup>27</sup> The delocalization process can also be clearly seen in Figs. 1(a) and 1(b), where  $\rho(T, B)$  decreases in the low temperature region when the magnetic field is increased to higher value, especially for  $x=0.12$ . We may even speculate that the second CP for  $x=0.09$  could exist in much more higher magnetic field that is beyond our present measuring ability. However, we should note that not all samples'  $\rho(T, B)$  curves cross well in certain  $(B, T)$  region possibly due to superconducting fluctuations, thermal fluctuation, and complicated backgrounds of HTSC.

In conclusion, the normal-state transport properties of LCCO thin films are systematically studied by applying high magnetic field to suppress the superconducting state. The heavily underdoped LCCO thin films show quite strong  $n$ -MR effect, while in the superconducting region, the LCCO thin films demonstrate a crossover from  $p$ -MR to  $n$ -MR around magnetic field  $B_{pn}$ , and the minimum  $n$ -MR is found

in the optimally doped region. For slightly underdoped ( $x=0.09$ ) LCCO thin films, the  $B_{pn}$  shows a parabolic relation with temperature. We argue that both field suppression of SDW gap and field-induced delocalization cause the  $n$ -MR behavior and result in this parabolic behavior of  $B_{pn}(T)$ . The slightly overdoped ( $x=0.12$ ) LCCO thin films show second crossing point of the  $\rho(T, B)$  curves, which is suggested to be the insulator-metal phase transition induced by high magnetic fields. We anticipate that much more high field will cause the oscillation of  $\rho(T, B)$ , which is similar to that of  $\text{YBa}_2\text{Cu}_3\text{O}_{6.5}$ ,<sup>30</sup> which may enlighten us on the subject of revealing the Fermi surface of electron-doped HTSC. These results can be used for a better understanding of LCCO and other electron-doped superconductors.

We thank B. Leridon for crucial discussion and F. Herlach for technique support. This work is supported by the MOST project (2004CB619004, 2006CB921802) and the National Natural Science Foundation of China, and the bilateral BIL China/Flaners Project. The work in Leuven is supported by the GOA, IAP, and FWO Projects.

\*brzhao@aphy.iphy.ac.cn

<sup>1</sup>Y. Ando, G. S. Boebinger, A. Passner, T. Kimura, and K. Kishio, Phys. Rev. Lett. **75**, 4662 (1995).

<sup>2</sup>N. Morozov, L. Krusin-Elbaum, T. Shibauchi, L. N. Bulaevskii, M. P. Maley, Y. I. Latyshev, and T. Yamashita, Phys. Rev. Lett. **84**, 1784 (2000).

<sup>3</sup>S. Ono, Y. Ando, T. Murayama, F. F. Balakirev, J. B. Betts, and G. S. Boebinger, Phys. Rev. Lett. **85**, 638 (2000).

<sup>4</sup>F. Rullier-Albenque, H. Alloul, C. Proust, P. Lejay, A. Forget, and D. Colson, Phys. Rev. Lett. **99**, 027003 (2007).

<sup>5</sup>P. C. Li, F. F. Balakirev, and R. L. Greene, Phys. Rev. Lett. **99**, 047003 (2007).

<sup>6</sup>G. S. Boebinger, Y. Ando, A. Passner, T. Kimura, M. Okuya, J. Shimoyama, K. Kishio, K. Tamasaku, N. Ichikawa, and S. Uchida, Phys. Rev. Lett. **77**, 5417 (1996).

<sup>7</sup>Y. Dagan, M. C. Barr, W. M. Fisher, R. Beck, T. Dhakal, A. Biswas, and R. L. Greene, Phys. Rev. Lett. **94**, 057005 (2005).

<sup>8</sup>M. A. Steiner, G. Boebinger, and A. Kapitulnik, Phys. Rev. Lett. **94**, 107008 (2005).

<sup>9</sup>Y. Dagan, M. M. Qazilbash, C. P. Hill, V. N. Kulkarni, and R. L. Greene, Phys. Rev. Lett. **92**, 167001 (2004).

<sup>10</sup>K. Jin, B. Y. Zhu, J. Yuan, H. Wu, L. Zhao, B. X. Wu, Y. Han, B. Xu, L. X. Cao, X. G. Qiu, and B. R. Zhao, Phys. Rev. B **75**, 214501 (2007).

<sup>11</sup>V. F. Gantmakher, S. N. Ernolov, G. E. Tsydynzhapov, A. A. Zhukov, and T. I. Baturina, JETP Lett. **77**, 424 (2003).

<sup>12</sup>N. P. Armitage, F. Ronning, D. H. Lu, C. Kim, A. Damascelli, K. M. Shen, D. L. Feng, H. Eisaki, Z. X. Shen, P. K. Mang, N. Kaneko, M. Greven, Y. Onose, Y. Taguchi, and Y. Tokura, Phys. Rev. Lett. **88**, 257001 (2002).

<sup>13</sup>H. Wu, L. Zhao, J. Yuan, L. X. Cao, J. P. Zhong, L. J. Gao, B. Xu, P. C. Dai, B. Y. Zhu, X. G. Qiu, and B. R. Zhao, Phys. Rev. B **73**, 104512 (2006).

<sup>14</sup>M. Naito, S. Karimoto, and A. Tsukada, Supercond. Sci. Technol. **15**, 1663 (2002).

<sup>15</sup>K. Jin, J. Yuan, L. Zhao, H. Wu, X. Y. Qi, B. Y. Zhu, L. X. Cao, X. G. Qiu, B. Xu, X. F. Duan, and B. R. Zhao, Phys. Rev. B **74**, 094518 (2006).

<sup>16</sup>L. Zhao, H. Wu, J. Miao, H. Yang, F. C. Zhang, X. G. Qiu, and B. R. Zhao, Supercond. Sci. Technol. **17**, 1361 (2004).

<sup>17</sup>The results will be discussed in detail elsewhere.

<sup>18</sup>P. Fournier, J. Higgins, H. Balci, E. Maiser, C. J. Lobb, and R. L. Greene, Phys. Rev. B **62**, R11993 (2000).

<sup>19</sup>T. Sekitani, M. Naito, and N. Miura, Phys. Rev. B **67**, 174503 (2003).

<sup>20</sup>M. Z. Cieplak, A. Malinowski, S. Guha, and M. Berkowski, Phys. Rev. Lett. **92**, 187003 (2004).

<sup>21</sup>A. Zimmers, J. M. Tomczak, R. P. S. M. Lobo, N. Bontemps, C. P. Hill, M. C. Barr, Y. Dagan, R. L. Greene, A. J. Millis, and C. C. Homes, Europhys. Lett. **70**, 225 (2005).

<sup>22</sup>Y. Onose, Y. Taguchi, K. Ishizaka, and Y. Tokura, Phys. Rev. Lett. **87**, 217001 (2001).

<sup>23</sup>M. A. Skvortsov and M. V. Feigel'man, Phys. Rev. Lett. **95**, 057002 (2005).

<sup>24</sup>T. I. Baturina, C. Strunk, M. R. Baklanov and A. Satta, Phys. Rev. Lett. **98**, 127003 (2007).

<sup>25</sup>To determine the upper critical field of all superconducting LCCO films and the method, it will be detailedly shown elsewhere.

<sup>26</sup>M. P. A. Fisher, G. Grinstein, and S. M. Girvin, Phys. Rev. Lett. **64**, 587 (1990).

<sup>27</sup>E. Bielejec and W. H. Wu, Phys. Rev. Lett. **88**, 206802 (2002).

<sup>28</sup>T. Wang, K. P. Clark, G. F. Spencer, A. M. Mack, and W. P. Kirk, Phys. Rev. Lett. **72**, 709 (1994).

<sup>29</sup>D. B. Haviland, Y. Liu, and A. M. Goldman, Phys. Rev. Lett. **62**, 2180 (1989).

<sup>30</sup>N. Doiron-Leyraud, C. Proust, D. LeBoeuf, J. Levallois, J.-B. Bonnemaison, R. X. Liang, D. A. Bonn, W. N. Hardy, and L. Taillefer, Nature (London) **447**, 565 (2007).